Multi-Carrier Chaos Shift Keying: System Design and Performance Analysis

Hua Yang, *Member, IEEE*, Wallace K. S. Tang, *Senior Member, IEEE*, Guanrong Chen, *Fellow, IEEE*, and Guo-Ping Jiang, *Senior Member, IEEE*

***Abstract*— Based on multi-carrier transmission and multi-level chaos shift keying modulation, a novel multi-carrier chaos shift keying (MC-CSK) modulation system is proposed and designed in this paper. The new system adopts multiple subcarriers, on which all chaotic basis signals along with multiple data-bearing signals are transmitted simultaneously. The data-bearing signals and their references, though sharing the same subcarriers, are separated by I/Q channels. As a consequence, the MC-CSK system can achieve higher bit rate and better spectral efficiency compared with the MC-DCSK system. It can also dispense with chaos synchronization and threshold shifting that are required in conventional CSK systems, and achieve a delay-line-free design in both transmitters and receivers. Also, the performance of the proposed system is further improved by normalizing all chaotic basis signals and making them strictly orthogonal using the Gram–Schmidt algorithm. Moreover, the bit error rates (BERs) of the MC-CSK system over additive white Gaussian noise and multi-path Rayleigh fading channels are derived. Finally, simulations are performed under different channel conditions and the effects of system parameters on the BER performance are evaluated. Both analytical and simulation results confirm that the MC-CSK system outperforms differential CSK (DCSK) and MC-DCSK systems in BER performance, except a rare case when the number of subcarriers is very small.**

***Index Terms*— Chaos-based communications, multi-carrier chaos shift keying, spectral efficiency, non-coherent detector, bit error rate.**

I. Introduction

DISTINGISHED for their excellent communication security, simplicity in circuit design, strong resistance to self-interference, low probability of interception and high robustness to multipath degradation, many chaos-based digital modulation schemes have been proposed, investigated and optimized in the past two decades [1]–[12]. The basic idea behind these schemes is to map binary/M-ary data symbols into different non-periodic and wideband chaotic basis signals.

Generally, the chaos-based digital modulation schemes can be classified as coherent and non-coherent schemes. For a coherent scheme, chaos synchronization is required and this stringent requirement is unfortunately impractical for real world applications. Therefore, schemes using non-coherent detectors are more popular. As a typical non-coherent system, differential chaos shift keying (DCSK) system [3] as well as its revised version named frequency-modulated differential chaos shift keying (FM-DCSK) system [4] has received great attention in recent years [13]–[20]. In both systems, transmitted-reference (T-R) technique is adopted to bypass the requirements of chaos synchronization and channel estimation. The data and reference signals are separated in a time division multiple access (TDMA) fashion, and therefore demodulation could be performed by evaluating correlations between the first and the second halves of the received signal in one symbol duration. Compared to other non-coherent systems, DCSK/FM-DCSK systems can achieve much better performances under various channel conditions [5]–[8], but at the cost of low data rate and low energy efficiency in general.

In order to increase the data rate or to obtain higher energy efficiency, several enhanced versions of DCSK have been designed, including quadrature chaos shift keying (QCSK) [9], multi-level DCSK/FM-DCSK [10], high-efficiency differential chaos shift keying (HE-DCSK) [11] and orthogonal chaotic vector shift keying (OCVSK) [12] systems. However, these solutions along with DCSK/FM-DCSK are not applicable to ultra wideband (UWB) communications because of the need for wideband delay lines. Implementing transceivers with wideband delay lines is practically difficult [21]. It will result in extremely high power consumption based on digital implementation, while analog wideband delay lines are too long and rather difficult to integrate with the CMOS technology.

To resolve the above difficulty in implementation, the wideband delay lines are removed from receivers in [22] and [23] by separating data and reference signals with different Walsh codes in the DCSK. Later, in [24], Walsh codes are substituted by chaotic codes to gain a higher data rate. For the similar purpose, a single carrier multi-level DCSK modulation system is proposed in [25], where Walsh codes and Hilbert transform are utilized to build multiple orthogonal basis functions. Differing from those in [22]–[24], however, the system in [25] separates

Manuscript received January 2, 2017; revised February 22, 2017; accepted March 13, 2017. Date of publication April 3, 2017; date of current version July 26, 2017. This work was supported in part by the National Natural Science Foundation of China under Grant 61401226 and Grant 61374180, in part by the Hong Kong Research Grants Council under Grant GRF CityU11234916, in part by the City University of Hong Kong under Grant 7004422, in part by the Jiangsu Government Scholarship for Oversea Studies, and in part by the University Science Research Project of Jiangsu Province under Grant 16KJB510045. This paper was recommended by Associate Editor G. Jovanovic Dolecek.

H. Yang is with the School of Electronic Science and Engineering, Nanjing University of Posts and Telecommunications, Nanjing 210023, China (e-mail: yangh@njupt.edu.cn).

W. K. S. Tang and G. R. Chen are with the Department of Electronic Engineering, City University of Hong Kong, Hong Kong (e-mail: eekstang@cityu.edu.hk; eegchen@cityu.edu.hk).

G.-P. Jiang is with the School of Automation, Nanjing University of Posts and Telecommunications, Nanjing 210023, China (e-mail: jianggp@njupt.edu.cn).

Color versions of one or more of the figures in this paper are available online at http://ieeexplore.ieee.org.

Digital Object Identifier 10.1109/TCSI.2017.2685344

data and reference signals not by codes but by two phases of a given sinusoidal carrier. Although no delay lines are needed by receivers in [22]–[25], there are more delay lines in the transmitters and extra code synchronization requirements also complicate the system design of these schemes.

To solve the delay line problem as well as to combat with the hostile propagation environments in high data rate mobile communications, multi-carrier (MC) transmission technique can be applied into chaos-based digital modulations so as to allow simultaneous transmissions of data and reference signals on multiple subcarriers. As an effective solution adopted by many recent standards, such as DVB-T, IEEE 802.11a, WiMAX, LTE and so on, MC shows great potentials in digital broadcasting, WLAN, UWB and many other mobile wireless broadband communications [26]–[29]. In the MC transmission, a serial high rate data stream is converted into many parallel low-rate sub-streams, where each one is carried by an allocated subcarrier. By using the fast Fourier transform (FFT) technique, MC modulation can be efficiently implemented in digital settings [30]. With a long symbol time, MC systems show great immunity to impulsive noise and delay spread, i.e., inter-symbol interference (ISI). In this way, combining MC transmission and chaos-based digital modulation not only can solve the delay line problem perfectly but also can inherit many merits that were originally reported from the multi-carrier spread spectrum (MC-SS) schemes [31], such as high spectral efficiency, robustness and flexibility.

The MC technique is first combined with DCSK in [32], where a new system called multi-carrier differential chaos shift keying (MC-DCSK) is suggested. Later, in [33], MC-DCSK is extended to multi-user scenarios, where all users share some predefined subcarriers for data transmission. Defined as a new cognitive multi-user access strategy, an analog network coding scheme is designed in [34] for MC-DCSK. In MC-DCSK, one of the subcarriers is assigned to the chaotic reference signal, while the others are assigned to multiple data-bearing signals, which share the same reference signal. In consequence, MC-DCSK increases both the data rate and the energy efficiency, resulting in better bit error rate (BER) performance as compared to DCSK. However, the spectral efficiency of MC-DCSK is relatively low since the data-bearing signal, occupying a certain subcarrier during one symbol period, carries only one single data bit each time.

To simultaneously fulfill the surged demands of higher spectral efficiency, better data security and higher data rate in mobile wireless communications, a novel multi-carrier chaos shift keying (MC-CSK) modulation system is designed in this paper. The proposed system is based on multi-level CSK, in which data-bearing signals are generated by mapping M-ary data symbols into normalized orthogonal chaotic basis signals. In each symbol duration, all the chaotic basis signals are being transmitted as the references on different subcarriers in the MC-CSK system, together with multiple data-bearing signals carrying different symbols. To be free of interference, these reference and data-bearing signals, though occupying same subcarriers, are separated by orthogonal I/Q channels. In this way, chaos synchronization and threshold shifting in conventional CSK system are eliminated in MC-CSK. Instead, a non-coherent detector that compares correlations between each received data-bearing signal and all chaotic basis signals can be utilized for data recovery. With one data-bearing signal carrying more data bits, the proposed MC-CSK system has much better spectral efficiency and a much higher data rate.

The rest of the paper is organized as follows. In Section II, the generation of chaotic basis signals in the proposed system is first introduced, and the transceiver architecture as well as the basis of the MC-CSK system is then described. In Section III, the BER performances of the MC-CSK system over additive white Gaussian noise (AWGN) and multipath Rayleigh fading channels are derived. Simulation results are reported with comparisons in Section IV. Finally, conclusions are given in Section V.

II. Multi-Carrier CSK System

In this section, the basis and the architecture of the MC-CSK system are presented. To start with, the design of the generator of chaotic basis signals is first presented.

A. Generator of Chaotic Basis Signals

In binary CSK modulation [1], two chaotic basis signals are utilized to represent two different binary symbols, respectively. Depending on which chaotic basis signal is received, binary symbols can be retrieved at the receiver side. This idea has been extended to multi-level CSK modulation, in which multiple dissimilar chaotic signals are used as basis signals to represent multiple M-ary symbols.

As far as system implementation is concerned, chaotic basis signals used in the MC-CSK system can be produced either from multiple distinct chaotic systems or from a chaotic system with different initials or bifurcation parameters. Nevertheless, the obtained chaotic basis signals have imperfections, i.e., their auto-correlations may vary from symbol to symbol and their cross-correlations also fluctuate around the zero value. As a result, the system performance is deteriorated, especially for small spreading factors. This negative effect escalates when more chaotic basis signals are involved, as in MC-CSK, impacting on the system performance despite having a relatively large spreading factor.

There are two possible solutions to improve the characteristics of auto-correlations and cross-correlations of the chaotic basis signals. The first solution is to combine the frequency modulator [4] and Hadamard-Walsh codes [35]. Since chaotic signals weighted by Walsh codes are strictly orthogonal, the values of their cross-correlations will always be zero. In addition, chaotic signals that undergo the frequency modulator have fixed power and subsequently can eliminate variations of auto-correlations. The second solution is based on the Gram-Schmidt algorithm [12]. Due to the fact that Walsh-based orthogonalization will introduce more additional delay lines in transmitters and could be invalid in multipath channels and asynchronous multiuser situations, only the Gram-Schmidt orthogonalization that needs no delay lines in system implementation is considered here.

To generate the chaotic basis signals for the MC-CSK system, an orthogonal chaotic signal generator (OCSG) is designed. Referring to the design block diagram in Fig. 1,

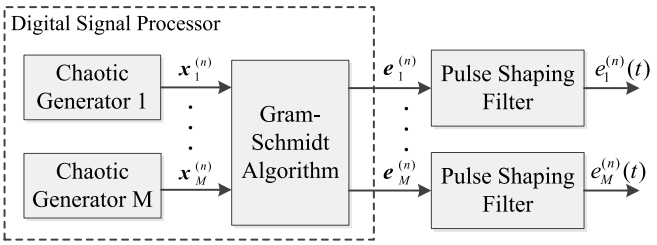

Fig. 1. Design block diagram of orthogonal chaotic signal generator.

every chaotic basis signal in a given symbol duration is constructed on the basis of a finite-length chaotic vector, which varies from symbol to symbol. In the n-th symbol duration, M chaotic generators generate M different chaotic vectors, $\boldsymbol{x}_1^{(n)}, \ldots, \boldsymbol{x}_M^{(n)}$, respectively. These chaotic generators could be implemented by realizing a particular chaotic attractor with different initials or bifurcation parameters in the digital signal processor (DSP). Using the same DSP, the Gram-schmidt algorithm is applied to the output vectors of these chaotic generators for the purposes of orthogonalization and normalization.

It is remarked that the Gram-Schmidt algorithm requires all input vectors be linearly independent. As proved in [8], the chaotic vectors $\boldsymbol{x}_1^{(n)}, \ldots, \boldsymbol{x}_M^{(n)}$ of infinite signal length are orthogonal and therefore linearly independent. For a finite signal length β, since chaotic system is highly sensitive to initial conditions and system parameters, the correlation coefficients of $\boldsymbol{x}_1^{(n)}, \ldots, \boldsymbol{x}_M^{(n)}$ tend to decay rapidly to nearly zero when β increases, making these vectors linearly independent. For illustration, consider a matrix $X \in R^{M\times\beta}$ defined as

$$X = \begin{bmatrix} \boldsymbol{x}_1^{(n)} \\ \boldsymbol{x}_2^{(n)} \\ \vdots \\ \boldsymbol{x}_M^{(n)} \end{bmatrix} \tag{1}$$

If $\boldsymbol{x}_1^{(n)}, \ldots, \boldsymbol{x}_M^{(n)}$ are linearly independent, the rank of X in (1) should be M. Figure 2 depicts the ranks of matrix X against β with different values of M. The results are based on 100,000 trials in which the logistic map $x_{i+1} = 1 - 2x_i^2$ used in [8] with M initials is employed and different initials are used in each trial. As shown in Fig. 2, when $\beta \geq M$, the rank of X equals M for all the trials, implying that the chaotic vectors $\boldsymbol{x}_1^{(n)}, \ldots, \boldsymbol{x}_M^{(n)}$ are linearly independent and therefore satisfy the condition required by the Gram-Schmidt algorithm. It should be emphasized that a similar condition is widely accepted and has been applied in the literature, e.g., in [5]–[12], [24], [32], [33], and [36].

Now, consider M different chaotic vectors generated by a particular chaotic system with M different initials in the n-th symbol duration, which can be described as

$$\boldsymbol{x}_j^{(n)} = [x_{j,n\beta+1}, x_{j,n\beta+2}, \ldots, x_{j,n\beta+\beta}], \quad \text{for } j = 1, \ldots, M \tag{2}$$

where $x_{j,n\beta+1}$ denotes the $(n\beta+1)$-th chaotic sample outputted by the chaotic generator with the j-th initial, and β is the number of chaotic samples in one symbol duration.

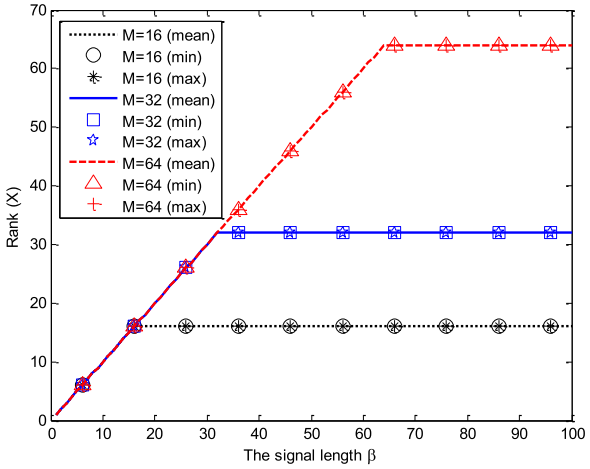

Fig. 2. Rank(X) against β for different values of M. The minimum, mean and maximum values of rank obtained in 100,000 trials are plotted for each case.

Choosing a relatively large β with $\beta \geq M$, chaotic vectors in (2) are linearly independent, satisfying the condition for the Gram-Schmidt algorithm. One can then obtain M orthogonal basis vectors $\boldsymbol{u}_1^{(n)}, \ldots, \boldsymbol{u}_M^{(n)}$ by the following Gram-Schmidt orthogonalization process:

$$\boldsymbol{u}_j^{(n)} = \begin{cases} \boldsymbol{x}_1^{(n)}, & \text{for } j = 1 \\ \boldsymbol{x}_j^{(n)} - \displaystyle\sum_{i=1}^{j-1} \frac{\left\langle \boldsymbol{x}_j^{(n)}, \boldsymbol{u}_i^{(n)} \right\rangle}{\left\langle \boldsymbol{u}_i^{(n)}, \boldsymbol{u}_i^{(n)} \right\rangle} \boldsymbol{u}_i^{(n)}, & \text{for } j = 2, \ldots, M \end{cases} \tag{3}$$

where $\left\langle \boldsymbol{x}_j^{(n)}, \boldsymbol{u}_i^{(n)} \right\rangle$ represents the inner product of vectors $\boldsymbol{x}_j^{(n)}$ and $\boldsymbol{u}_i^{(n)}$, which is given by

$$\left\langle \boldsymbol{x}_j^{(n)}, \boldsymbol{u}_i^{(n)} \right\rangle = \sum_{m=1}^{\beta} x_{j,n\beta+m} u_{i,n\beta+m} \tag{4}$$

and $u_{i,n\beta+m}$ is the m-th element of vector $\boldsymbol{u}_i^{(n)}$.

The orthogonal vectors in (3) will be further normalized to have unity energy, such that

$$\boldsymbol{e}_j^{(n)} = \frac{\boldsymbol{u}_j^{(n)}}{\sqrt{\left\langle \boldsymbol{u}_j^{(n)}, \boldsymbol{u}_j^{(n)} \right\rangle}}, \quad \text{for } j = 1, \ldots, M \tag{5}$$

where $\boldsymbol{e}_j^{(n)}$ is referred to as the j-th normalized orthogonal vector in the n-th symbol duration.

For demonstration, 64 chaotic vectors are obtained from the logistic map in [8] with 64 different initials. Fig. 3 depicts the histograms of auto-correlations and cross-correlations of these chaotic vectors before and after the Gram-Schmidt algorithm. As shown, before the Gram-Schmidt algorithm, variations exist in both auto-correlations and cross-correlations, leading to more uncertainties in decision variables. Fortunately, these variations are removed perfectly by applying the Gram-Schmidt algorithm. It is remarked that the normalized orthogonal vectors $\boldsymbol{e}_1^{(n)}, \ldots, \boldsymbol{e}_M^{(n)}$ in (5) are still chaotic, confirmed with the positive largest Lyapunov exponents obtained by the method proposed in [37] as shown in Fig. 4.

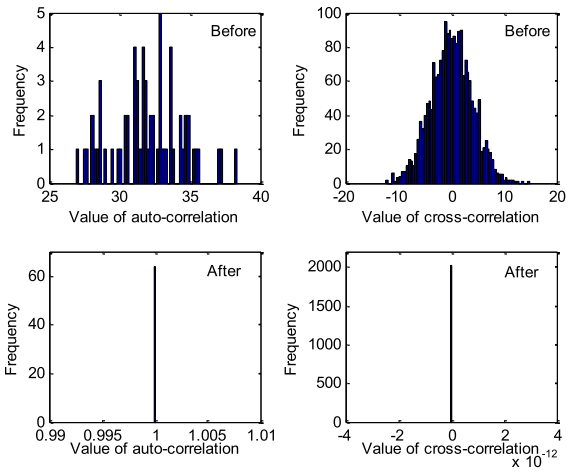

Fig. 3. Histograms of auto-correlations and cross-correlations of chaotic vectors before and after Gram-Schmidt orthogonalization ($\beta = 64$ and $M = 64$).

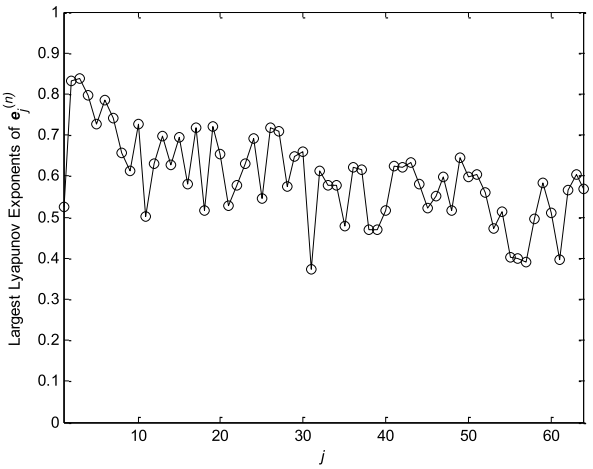

Fig. 4. The largest Lyapunov exponents of normalized orthogonal vectors in (5) with $\beta = 3000$ and $M = 64$.

Finally, the chaotic basis signals are obtained by filtering the M normalized orthogonal vectors $\boldsymbol{e}_1^{(n)}, \ldots, \boldsymbol{e}_M^{(n)}$ that are outputted by the DSP unit with M identical pulse shaping filters.

Let $\boldsymbol{e}_j^{(n)} = [e_{j,n\beta+1}, e_{j,n\beta+2}, \ldots, e_{j,n\beta+\beta}]$ be the j-th normalized orthogonal vector in the n-th symbol duration. Then, the corresponding chaotic basis signal is represented by

$$e_j^{(n)}(t) = \sum_{k=n\beta+1}^{n\beta+\beta} e_{j,k} h_T(t - kT_c), \quad \text{for } j = 1, \ldots, M \tag{6}$$

where T_c is the chip time and $h_T(t)$ is the impulse response of the pulse shaping filter.

In the design, a square-root-raised cosine filter with roll-off factor α ($0 < \alpha \leq 1$) is adopted for pulse shaping. The frequency spectrum of $h_T(t)$ is limited to $[-\Delta f/2, \Delta f/2]$ with $\Delta f = (1+\alpha)/T_c$ and the energy of $h_T(t)$ is normalized to unity:

$$\int_0^{T_c} h_T^2(t)dt = 1 \tag{7}$$

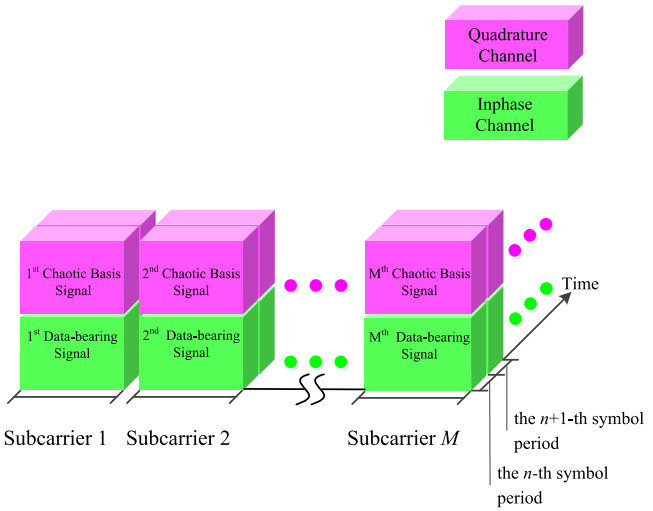

Fig. 5. Format of the signal transmitted in the MC-CSK system during the n-th symbol period.

B. Basis of MC-CSK

The main feature of the MC-CSK system is that it introduces both MC transmission technique and T-R technique into multi-level CSK modulation. The former technique not only increases the attainable bit rate and spectral efficiency but also avoids using wideband delay lines in the transceiver design, while the latter avoids both the threshold shifting problem and using chaotic synchronization circuit in the receiver design.

In the MC-CSK system, M subcarriers are employed to transmit multiple data symbols in a parallel way so that a higher data rate could be achieved. As a T-R based system, MC-CSK transmits M chaotic basis signals (see (6)) as the reference signals over the Quadrature channel on these M subcarriers, respectively, during one symbol period. Meanwhile, M data-bearing signals carrying M different data symbols are transmitted over the Inphase channel by the same subcarriers. As a result, chaos synchronization circuit is not needed by this receiver since the reference signals, i.e. the chaotic basis signals, are available. In addition, wideband delay line is not needed either, since the reference and data-bearing signals are separated over orthogonal I/Q channels. For visualization, Fig. 5 shows the format of the transmitted signal during the n-th symbol period in the MC-CSK system.

At the receiver side, M chaotic basis signals and M data-bearing signals are extracted from the Quadrature and Inphase channels of all subcarriers. To recover a certain data symbol, the recovered data-bearing signal is correlated with all M extracted chaotic basis signals and decision will be made in favor of the largest correlator output for achieving optimal detection performance.

C. Transmitter

Fig. 6 depicts a feasible structure of the MC-CSK transmitter. In the n-th symbol duration, serial bits $b_1^{(n)} \ldots b_{M\log_2 M}^{(n)}$ are converted into M parallel bit sequences representing data symbols, $a_1^{(n)}, \ldots, a_M^{(n)}$, by the serial to parallel circuit. Each data symbol is defined as a bit sequence consisting

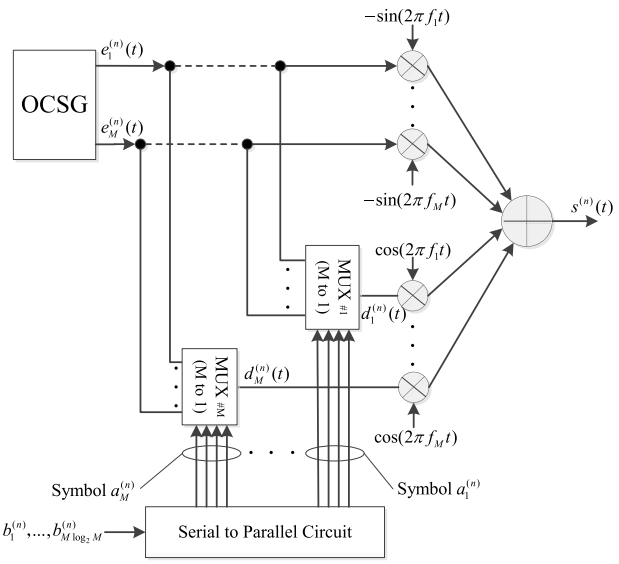

Fig. 6. Block diagram of the MC-CSK transmitter.

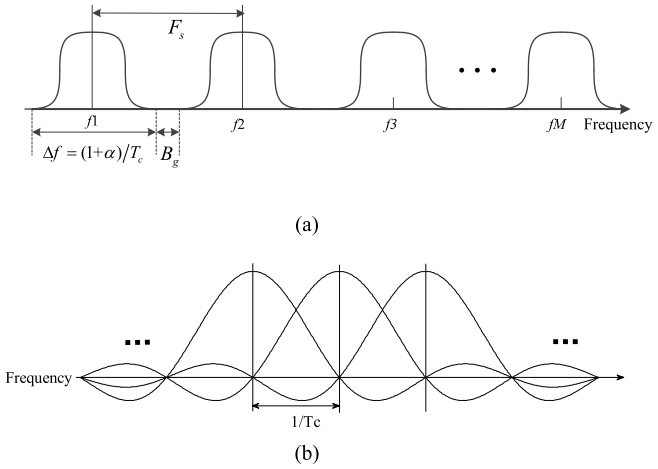

Fig. 7. Power spectrum of the transmitted MC-CSK signal. (a) FDM filtering with guard bands. (b) OFDM with overlapped sub-bands.

of $\log_2 M$ bits. Referring to Fig. 6, the i-th data symbol is given by

$$a_i^{(n)} = \left(b_{(i-1)\log_2 M+1}^{(n)} \cdots b_{i\log_2 M}^{(n)}\right), \quad \text{for } i = 1, \ldots, M \quad (8)$$

where $b_{(i-1)\log_2 M+1}^{(n)} \in \{0, 1\}$ is the least significant bit (LSB) of the i-th data symbol transmitted in the n-th symbol duration.

In the MC-CSK system, every chaotic basis signal in (6) corresponds to one of these M-ary data symbols. The mapping is simply performed by an M-to-1 multiplexer (MUX) as shown in Fig. 6, where its output is addressed by the data symbols. Mathematically, one has

$$d_i^{(n)}(t) = e_j^{(n)}(t), \quad \text{if } dec\left[a_i^{(n)}\right] = j, \text{ for } i = 1, \ldots, M \quad (9)$$

where $d_i^{(n)}(t)$ represents the data-bearing signal carrying data symbol $a_i^{(n)}$, $dec[\cdot]$ denotes a binary-to-decimal converting operator defined as

$$dec\left[a_i^{(n)}\right] = 1 + \sum_{k=1}^{\log_2 M} b_{(i-1)\log_2 M+k}^{(n)} \cdot 2^{k-1} \quad (10)$$

For parallel and simultaneous transmission, transmitter will modulate the obtained data-bearing signals $d_1^{(n)}(t), \ldots, d_M^{(n)}(t)$ onto the Inphase sinusoidal carriers with center frequencies of $f_1, f_2, \ldots, f_M$, respectively, while the chaotic basis signals $e_1^{(n)}(t), \ldots, e_M^{(n)}(t)$ in current symbol duration are also modulated onto the Quadrature sinusoidal carriers with same center frequencies.

Finally, these modulated signals are summed and transmitted by the MC-CSK transmitter in Fig. 6. The transmitted signal in the n-th symbol duration is then presented by

$$s^{(n)}(t) = \sum_{i=1}^{M} d_i^{(n)}(t)\cos(2\pi f_i t) - \sum_{i=1}^{M} e_i^{(n)}(t)\sin(2\pi f_i t) \quad \text{for } n\beta T_c < t \le (n+1)\beta T_c \quad (11)$$

where f_i is the center frequency corresponding to the i-th subcarrier and is defined as $f_i = f_0 + iF_s$. Here, F_s is the frequency spacing between adjacent subcarriers, and f_0 is the fundamental carrier frequency satisfying $f_0 \gg 1/T_c$.

D. Spectral Efficiency

To evaluate the spectral efficiency of the proposed scheme, Fig. 7 shows the power spectrum of the transmitted MC-CSK signals with M subcarriers. Two different cases are considered here.

In Fig. 7(a), the conventional frequency division multiplexing (FDM) technique is borrowed and filters are used to separate the sub-bands completely. Since band overlapping will cause inter-carrier interference (ICI), it is assumed that $F_s \ge \Delta f$ so that all sub-bands are disjointed. This is a common assumption used in MC transmission [32]. Clearly, in this case, the ICI can be avoided as the spectra of different subcarrier channels are non-overlapping and separated by the guard band B_g ($B_g \ge 0$). Although the spectral efficiency is lowered due to guard bands, the difficulty of implementing very sharp filters can be avoided.

Another case, which is based on orthogonal frequency division multiplexing (OFDM), is shown in Fig. 7(b). Actually, OFDM is a special case of MC transmission. In this case, all subcarriers are orthogonal over each chip duration, implying that cross-talk between subcarriers is eliminated and hence inter-carrier guard bands are not required. The frequency spacing F_s is then reduced to $1/T_c$. Time-limited rectangular pulse shaping is used in OFDM, thus the individual spectra are sinc functions, as shown in Fig. 7 (b). With band overlapping, the spectral efficiency of OFDM is increased. Although the spectra are overlapped, the signals can still be separated in the receiver, not by filters but by Discrete Fourier Transform (DFT) [30]. However, due to the carrier frequency offset caused by motion-induced Doppler effects and frequency mismatches of local oscillators in transmitter and receiver, the orthogonality among all the subcarriers in OFDM might be damaged, thus resulting in ICI. As ICI

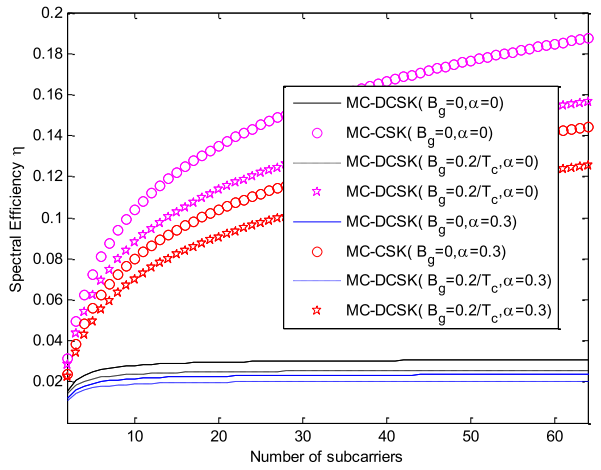

Fig. 8. Spectral efficiency for various numbers of subcarriers with $\beta = 32$.

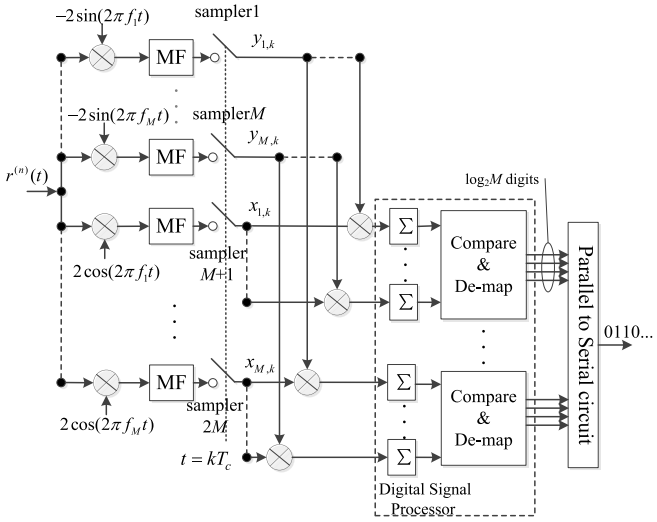

Fig. 9. Design block diagram of the MC-CSK receiver.

may degrade the BER performance severely, many methods have been proposed in OFDM to effectively combat ICI, e.g. by inserting an appropriate cyclic prefix between adjacent symbols [26], frequency offset estimation and compensation [38], [39], ICI equalization [40], and so on.

From Fig. 7(a), the total required bandwidth (B) in the MC-CSK system is calculated by

$$B = M\frac{(1+\alpha)}{T_c} + (M-1)\,B_g \tag{12}$$

The spectral efficiency as defined in [41] can be computed by

$$\eta_{\text{MC-CSK}} = \frac{\text{bit rate}}{\text{total bandwidth}} = \frac{\frac{M\log_2 M}{\beta T_c}}{M\frac{(1+\alpha)}{T_c} + (M-1)\,B_g} \tag{13}$$

Similarly, the spectral efficiency of MC-DCSK system is

$$\eta_{\text{MC-DCSK}} = \frac{\frac{M-1}{\beta T_c}}{M\frac{(1+\alpha)}{T_c} + (M-1)\,B_g} \tag{14}$$

Since the guard band B_g is typically much smaller than $1/T_c$, (13) and (14) could be approximated and become (15) and (16), respectively, for a large M.

$$\eta_{\text{MC-CSK}} \approx \frac{\log_2 M}{(1+\alpha)\beta} \tag{15}$$

$$\eta_{\text{MC-DCSK}} \approx \frac{1}{(1+\alpha)\beta} \tag{16}$$

Note that, with $\alpha = 0$, (15) and (16) can also be used respectively to evaluate the spectral efficiencies of MC-CSK and MC- DCSK systems for the OFDM case given in Fig. 7(b).

With some fixed values of β, Fig. 8 compares the spectral efficiencies of these two systems. Since multiple data bits are carried by a single subcarrier in the MC-CSK system, the spectral efficiency of MC-CSK is about $\log_2 M$ times as big as that of MC-DCSK. This is confirmed by the results shown in Fig. 8, demonstrating the outperformance of MC-CSK. It is also apparent that both MC-CSK and MC-DCSK systems gain their best spectral efficiencies due to minimal total bandwidth when $\alpha = 0$ and $B_g = 0$. If the guard band grows, their spectral efficiencies decrease, matching with the earlier analyses given in (13) and (14).

E. Receiver

Fig. 9 shows the block diagram of the MC-CSK receiver, where a differential correlation detection method is employed.

In this design, the received signal $r^{(n)}(t)$ will first be multiplied with the synchronized Quadrature and Inphase carriers of the M subcarriers, respectively. The resultant signals will then be fed into $2M$ identical matched filters (MF) separately. Here, matched filters, rather than low pass filters, are employed to maximize the output peak signal-to-noise ratio at each sampling time $t = kT_c$, and these filters should be matched to the pulse signal $h_T(t)$. The outputs of the upper M samplers are regarded as the estimated sequences of M chaotic basis signals, while the outputs of the bottom M samplers are regarded as the estimated data-bearing sequences transmitted on M subcarriers.

Correlations will be performed between each estimated data-bearing sequence and all the M estimated chaotic basis signal sequences, over the chaotic sequence of length β (Note: the blocks with symbol Σ in Fig. 9 are the correlation functions, which can be easily implemented with DSP). For each data-bearing signal sequence, the values of all relevant correlations will be compared and a decision in favor of the largest correlation value will be made. Later, data symbol (i.e., bit sequence) carried by this data-bearing signal sequence will be determined according to the opposite of the modulation rule given in (9). These operations can be completed by digital signal processors. Finally, the resultant M bit sequences will undergo the parallel-to-serial circuit so that the original serial data bits could be recovered.

III. Performance Analysis

In this section, the BER performance of MC-CSK system is analyzed over multipath Rayleigh fading channel as well as AWGN channel. The multipath Rayleigh fading channel model

in [42] is assumed. This model consists of L independent and identically distributed (i.i.d.) Rayleigh slow-fading channels, which is commonly used in the analysis of spread-spectrum wireless communication systems [16], [22], [25], [32], [43].

Since the channel is slow and flat fading, the propagation gain for each path can be regarded as constant during the whole symbol duration. Consider the transmission of symbols in the n-th symbol duration, on which the output of such an L-path Rayleigh slow fading channel is given by

$$r_n(t) = \sum_{p=1}^{L} \lambda_p^{(n)} s_n(t - \tau_p T_c) + \varepsilon(t) \tag{17}$$

where τ_p and $\lambda_p^{(n)}$ are the time delay and propagation gain of the p-th path affecting data symbols transmitted in the n-th symbol duration, respectively, and $\varepsilon(t)$ is stationary Gaussian noise with zero mean and power spectral density of $N_0/2$.

The propagation gains in all L paths are assumed to be independent random variables, while their probability density functions (PDF) are defined as

$$f_\lambda(z) = \frac{z}{E[\lambda^2]} e^{-\frac{z^2}{2E[\lambda^2]}} \tag{18}$$

where $E[\cdot]$ denotes the expectation operator and $E\left[\lambda^2\right]$ is the average propagation gain.

Assuming that both the sinusoidal carrier and the chip are perfectly synchronized, the estimated j-th chaotic basis signal sequence (i.e., the output of the j-th sampler in Fig. 9) can be derived as

$$y_{j,k} = \sum_{\substack{p=1 \\ k-n\beta-\tau_p \geq 0}}^{L} \lambda_p^{(n)} e_{j,k-\tau_p} + \underbrace{\sum_{\substack{p=1 \\ k-n\beta-\tau_p < 0}}^{L} \lambda_p^{(n-1)} e_{j,k-\tau_p-\beta}}_{\text{inter-symbol interference}} + \xi_{j,k} \quad \text{for } n\beta < k \leq (n+1)\beta \tag{19}$$

where $\xi_{j,k}$ is the k-th sample of the Gaussian noise added to the j-th reference signal.

Similarly, the estimated data-bearing signal sequence obtained from the i-th subcarrier (i.e., the output of the $(M+i)$-th sampler in Fig. 9) can be derived as

$$x_{i,k} = \sum_{\substack{p=1 \\ k-n\beta-\tau_p \geq 0}}^{L} \lambda_p^{(n)} d_{i,k-\tau_p} + \underbrace{\sum_{\substack{p=1 \\ k-n\beta-\tau_p < 0}}^{L} \lambda_p^{(n-1)} d_{i,k-\tau_p-\beta}}_{\text{inter-symbol interference}} + \zeta_{i,k} \quad \text{for } n\beta < k \leq (n+1)\beta \tag{20}$$

where $\zeta_{i,k}$ is the k-th sample of the Gaussian noise added to the data-bearing signal transmitted on the i-th subcarrier.

Subsequently, correlation between the estimated i-th data-bearing signal sequence and the recovered j-th chaotic basis signal sequence is computed by

$$C(i,j) = \sum_{k=n\beta+1}^{(n+1)\beta} x_{i,k} y_{j,k} \quad \text{for } 1 \leq i,\ j \leq M \tag{21}$$

It is assumed that the path delay τ_p is much smaller than the chaotic sequence length β, i.e., $0 < \tau_p \ll \beta$, which is common in many practical applications [43]. In this case, the inter-symbol interference (ISI) terms in (19) and (20) play a negligible role in correlation computation in (21). By ignoring ISI, (21) can be approximated by:

$$C(i,j) \approx \sum_{k=n\beta+1}^{(n+1)\beta} \left(\sum_{p=1}^{L} \lambda_p^{(n)} d_{i,k-\tau_p} + \zeta_{i,k} \right) \times \left(\sum_{p=1}^{L} \lambda_p^{(n)} e_{j,k-\tau_p} + \xi_{j,k} \right) \tag{22}$$

For any i with $i = 1, \ldots, M$, we first assume that $a_i^{(n)}$ being transmitted over the i-th subcarrier satisfies $dec\left[a_i^{(n)}\right] = i$. According to the modulation rule defined in (9), $d_{i,k-\tau_p}$ in (22) can be substituted by $e_{i,k-\tau_p}$. As demonstrated in [32] and [43] for the case of large β, one has

$$\sum_{k=n\beta+1}^{(n+1)\beta} e_{i,k-\tau_p} e_{j,k-\tau_q} \approx 0 \quad \text{for } p \neq q \tag{23}$$

Then, (22) becomes

$$C(i,j) \approx \sum_{k=n\beta+1}^{(n+1)\beta} \left(\sum_{p=1}^{L} \left(\lambda_p^{(n)}\right)^2 e_{i,k-\tau_p} e_{j,k-\tau_p} + \sum_{p=1}^{L} \lambda_p^{(n)} e_{i,k-\tau_p} \xi_{j,k} + \sum_{p=1}^{L} \lambda_p^{(n)} e_{j,k-\tau_p} \zeta_{i,k} + \zeta_{i,k} \xi_{j,k} \right) \tag{24}$$

Since the vectors in (5) are normalized and orthogonal to each other, (24) can finally be simplified as

$$\mathrm{C}(i,j) \approx \begin{cases} E_s \sum_{p=1}^{L} \left(\lambda_p^{(n)}\right)^2 + \sum_{k=n\beta+1}^{(n+1)\beta} \times \left(\sum_{p=1}^{L} \lambda_p^{(n)} e_{i,k-\tau_p} (\xi_{i,k} + \zeta_{i,k}) + \zeta_{i,k} \xi_{i,k} \right), & \text{if } i = j \\ \sum_{k=n\beta+1}^{(n+1)\beta} \left(\sum_{p=1}^{L} \lambda_p^{(n)} e_{i,k-\tau_p} \xi_{j,k} + \sum_{p=1}^{L} \lambda_p^{(n)} e_{j,k-\tau_p} \zeta_{i,k} + \zeta_{i,k} \xi_{j,k} \right), & \text{if } i \neq j \end{cases} \tag{25}$$

where E_s is the transmitted symbol energy in MC-CSK system. Since a data symbol is represented by $\log_2 M$ data bits, it follows that $E_b = E_s / \log_2 M$, where E_b is the bit energy of the transmitted signal.

For a given set of $(\lambda_1^{(n)}, \lambda_2^{(n)}, \ldots, \lambda_L^{(n)})$, $C(i,j)$ in (25) follows a Gaussian distribution with conditional mean value and

variance given, respectively, by

$$E\left[C(i,j)\right] = \begin{cases} E_s \sum_{p=1}^{L} \left(\lambda_p^{(n)}\right)^2, & \text{if } i = j \\ 0, & \text{if } i \neq j \end{cases} \quad (26)$$

$$\text{var}\left[C(i,j)\right] = 2E_s N_0 \sum_{p=1}^{L} \left(\lambda_p^{(n)}\right)^2 + \beta N_0^2 \quad (27)$$

where $\text{var}[\cdot]$ denotes the variance operator.

Since decisions are made in favor of the largest correlator output at the MC-CSK receiver, the probability of making a wrong decision for symbol $a_i^{(n)}$ can be derived as

$$P_i = 1 - prob\left(\max\{C(i,j), 1 \le j \le M\} = C(i,i)\right) \quad (28)$$

For $i \neq j$, correlations in (25) are independent and share the same distribution. Thus, the probability specified in (28) could be calculated by

$$P_i = 1 - \int_{-\infty}^{+\infty} \left(prob\left(C(i,j) < r, j \neq i | C(i,i) = r\right)\right)^{M-1} \times f(r)\, dr \quad (29)$$

in which

$$f(r) = \frac{1}{\sqrt{2\pi\, \text{var}\left[C(i,i)\right]}} e^{-\frac{(r - E[C(i,i)])^2}{2\text{var}[C(i,i)]}} \quad (30)$$

The error probabilities for $dec\left[a_i^{(n)}\right] \neq i$ can be derived in a similar way and they turn out to be identical to (29). In consequence, the probability in (29) could be used to represent the symbol error probability conditioned on $(\lambda_1^{(n)}, \lambda_2^{(n)}, \ldots, \lambda_L^{(n)})$ for any i-th subcarrier.

Denoting $\gamma_p = \left(\lambda_p^{(n)}\right)^2 E_b/N_0$ and $\gamma_b = \sum_{p=1}^{L} \gamma_p$, the overall conditional symbol error rate for a certain set of $(\lambda_1^{(n)}, \lambda_2^{(n)}, \ldots, \lambda_L^{(n)})$ is derived by

$$P_{\text{Symbol}}(\gamma_b) = \int_{-\infty}^{+\infty} \frac{1}{\sqrt{\pi}} \left\{1 - \left(1 - \frac{1}{2} erfc(r)\right)^{M-1}\right\} \times e^{-\left(r - \frac{\log_2 M}{\sqrt{\frac{4\log_2 M}{\gamma_b} + \frac{2\beta}{\gamma_b^2}}}\right)^2} dr \quad (31)$$

where $erfc(\cdot)$ denotes the complementary error function [44].

Given that $E\left[\gamma_1\right] = E\left[\gamma_2\right] = \cdots = E\left[\gamma_L\right] = \bar{\gamma}$, following the derivation in [45], the PDF of γ_b is calculated by

$$p(\gamma_b) = \frac{\gamma_b^{L-1}}{(L-1)!\bar{\gamma}^L} e^{-\frac{\gamma_b}{\bar{\gamma}}} \quad (32)$$

For the case that the propagation gains of L paths are different, $p(\gamma_b)$ is specified by

$$p(\gamma_b) = \sum_{p=1}^{L} \frac{1}{\bar{\gamma}_p} \prod_{j=1, j\neq p}^{L} \frac{\bar{\gamma}_p}{\bar{\gamma}_p - \bar{\gamma}_j} e^{-\frac{\gamma_b}{\bar{\gamma}_p}} \quad (33)$$

with $\overline{\gamma}_p = E\left[\gamma_p\right]$.

Based on the general relationship between the bit error probability and the symbol error probability reported in [45], the BER formula for MC-CSK over multipath Rayleigh fading channel can be obtained, as

$$BER_{\text{MC-CSK}} = \frac{M}{2(M-1)} \int_0^{+\infty} P_{\text{Symbol}}(\gamma_b) \times p(\gamma_b) d\gamma_b \quad (34)$$

Note that, with $L = 1$ and $\gamma_b = E_b/N_0$, formula (34) can also be used to evaluate the BER performance of MC-CSK over AWGN channel.

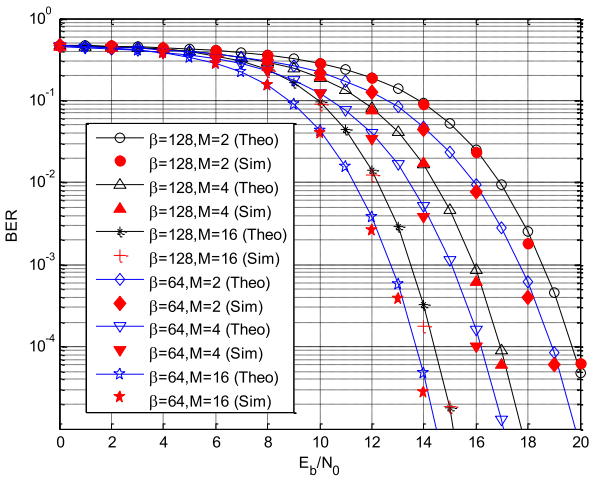

Fig. 10. Comparison between the simulated and analytical performances of MC-CSK with $\beta = 64$ and $\beta = 128$ for different M over AWGN channel.

IV. Simulation Results and Discussions

In this section, the performances of the MC-CSK system with various system parameters and under different channel conditions are evaluated based on extensive Monte Carlo simulations. The results will be directly compared to those of MC-DCSK, DCSK, and the four systems proposed in [16], [24], [25], and [33], respectively.

In all of the studied systems, chaotic sequences are generated by the logistic map $x_{i+1} = 1 - 2x_i^2$ [8]. In MC-DCSK and MC-CSK systems, the square-root-raised cosine pulse waveform with a roll-off factor $\alpha = 0.25$ is used for pulse shaping. It is also letting that, the total required bandwidth $B = 4M$Hz with guard band $B_g = 0$ and the symbol duration time $T_s = 640\mu$s. Since $T_s = \beta T_c$ and based on (12), the chaotic sequence length is thus given by $\beta = T_s B/M(1+\alpha)$.

A. Performance Evaluation

Firstly, the bit error rate formula (34), derived from the theoretical analysis in Sect. III, is validated. The simulated and analytical performance of MC-CSK over AWGN channel and over multipath Rayleigh fading channels with identical and different average power gains are obtained and the results are shown in Figs. 10-12, respectively. A very good agreement is clearly observed between the analytical predictions and the simulated results, confirming the theoretical analysis.

It clearly shows in Fig. 10 that, with a fixed β, the BER performance of MC-CSK over AWGN channel keeps improving when more subcarriers are involved. Similar phenomenon can be observed from Fig. 11 and Fig. 12 for the multipath

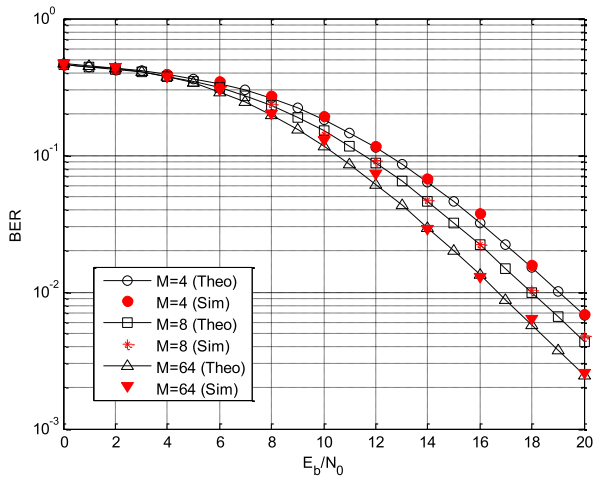

Fig. 11. Simulated and analytical BER performances of MC-CSK with $\beta = 64$ over two-paths Rayleigh fading channel ($L = 2$) with delays: $\tau_1 = 0$, $\tau_2 = 3$ and identical average power gains: $E[\lambda_1^2] = E[\lambda_2^2] = 1/2$.

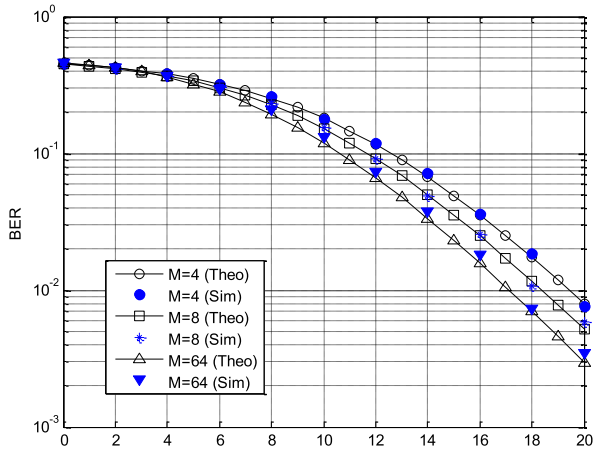

Fig. 12. Simulated and analytical BER performances of MC-CSK with $\beta = 64$ over two-paths Rayleigh fading channel ($L = 2$) with delays: $\tau_1 = 0$, $\tau_2 = 3$ and different average power gains: $E[\lambda_1^2] = 1/3$, $E[\lambda_2^2] = 2/3$.

Rayleigh fading channels. This is mainly attributed to the noise reduction in decision variables by using more orthogonal chaotic basis signals to represent more data bits. To further evaluate the impact of subcarrier number M on the BER performance of MC-CSK, Fig.13 plots the signal-noise ratio versus the number of subcarriers at BER level of 10^{-3}, 10^{-4} and 10^{-5}. As shown, BER performance improvement induced by M tends to decline with M, and becomes unobvious when $M \geq \beta/2$.

The effect of the chaotic sequence length β on the performance of MC-CSK is shown in Fig. 14 under various signal-to-noise ratios over AWGN channel. It is reported in [5] and [32] that, when β increases, the bit error rates of DCSK and MC-DCSK first drop and then tend to rise. This observation reflects the trade-off between weakening fluctuations in bit energy and increasing noise interferences in decision variables. However, as shown in Fig. 14, the performance of MC-CSK monotonically degrades as the length of the chaotic sequence increases, which is probably attributed to the removal of the varied auto-correlation of chaotic basis vectors in MC-CSK.

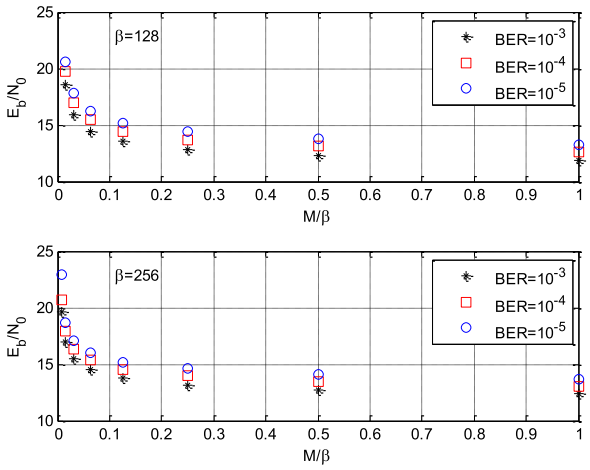

Fig. 13. The signal-noise ratio versus the number of subcarriers M at various BER levels for MC-CSK over AWGN channel.

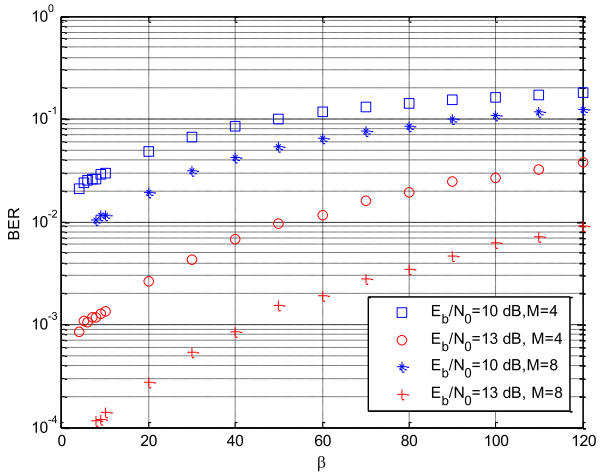

Fig. 14. Relationship between bit error rate and length β of chaotic sequence for MC-CSK over AWGN channel.

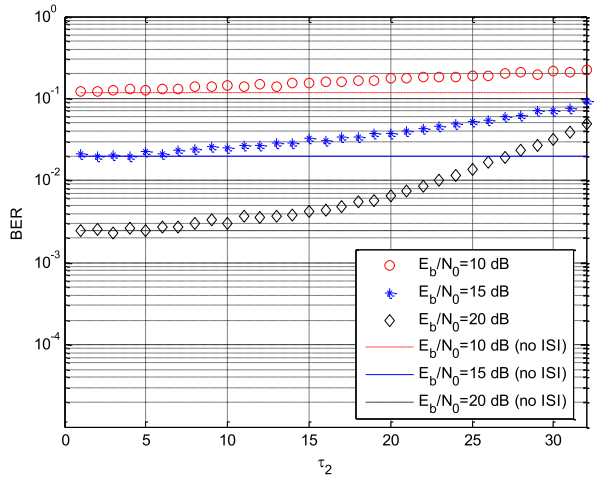

Fig. 15. Simulated effect of time delay τ_2 on the BER performance of MC-CSK over two-path Rayleigh fading channels with $\tau_1 = 0$ and equal average gain powers.

The last task of this subsection is to investigate the effect of time delay on BER performance over multipath fading channels. Fig. 15 shows the simulated BER performances of

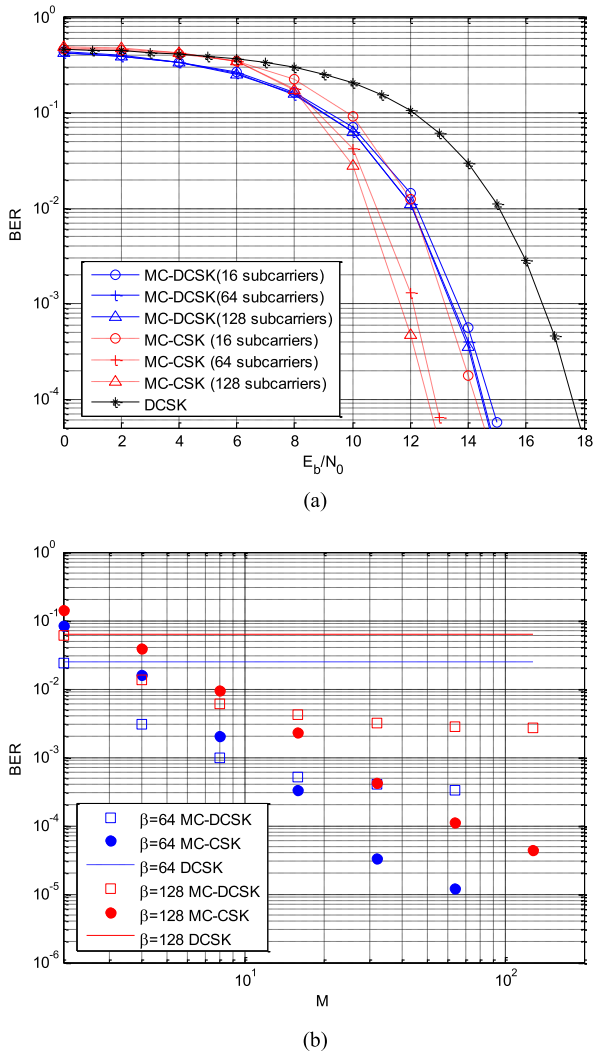

Fig. 16. BER comparison among MC-CSK, MC-DCSK and DCSK over AWGN channel. (a) $\beta = 128$. (b) $E_b/N_0 = 13dB$.

MC-CSK for different values of time delays in the second path (τ_2) of two-path Rayleigh fading channel, where $\tau_1 = 0$, $\beta = 64$ and $M = 64$. When the time delay is much smaller than the symbol duration, the simulated performances match the analytical ones quite well. It is because, with a small delay time τ_2, the ISI being neglected in (22) is so small that it has nearly no effect on the system performance. However, when τ_2 increases, the negative impact from ISI will be strengthened, and it is no longer negligible. As a result, disagreement between the simulated and analytical curves is noticed, say when $\tau_2 > 10$. Besides, this kind of disagreement becomes more apparent under the condition of a higher signal-to-noise ratio, since ISI plays a more significant role in BER performance when noise interference is relatively small.

B. Comparisons with Other Systems

For performance comparison, MC-CSK, MC-DCSK and DCSK systems are first simulated with different system parameters over AWGN channel. Figs. 16 (a) and (b) depict the results under the conditions of $\beta = 128$ and $E_b/N_0 = 13dB$, respectively. As shown in Fig. 16(b), the BER of DCSK is independent of the number of subcarriers, M, because there is no multi-carrier transmission in DCSK. In contrast, monotonic increments of performances against the number of subcarriers are noted for both MC-DCSK and MC-CSK.

It can also be observed in Figs. 16 that MC-CSK always shows better performance than DCSK if the number of subcarriers M is larger than 2. This performance superiority appears more and more evident (up to more than 5dB at BER level of 10^{-4}) when more subcarriers are used. Similarly, MC-CSK outperforms MC-DCSK when $M > 9$. For instance, when $M = 128$, MC-CSK shows about 2dB gain at BER level of 10^{-4} in comparison with MC-DCSK. These phenomena are resulted from the interaction of the positive and negative effects brought by multi-level CSK. On one hand, distance between any two symbol points in the constellation of multi-level CSK has been reduced to $\sqrt{2}/2$ times smaller than that in DCSK or MC-DCSK. This makes MC-CSK more sensitive to the channel noise and eventually degrades the system BER performance for a situation where M is small. On the other hand, for fixed E_b/N_0, increasing M implies that more orthogonal basis signals are employed to represent more symbols. This helps to reduce the noise interferences in decision variables expressed in (21) and to improve the BER performance of MC-CSK. However, when M equals or exceeds $\beta/2$, the noise reduction induced by M becomes unobvious, as shown in Fig. 13. For this reason, the performance curves of MC-CSK come closer when $M = 64$ or $M = 128$, as can be observed in Fig. 16(a). It should also be noted that, in most cases, MC transmission systems employ more than 64 and up to 2048 subcarriers [26]. For example, 2048 subcarriers are used in IEEE 802.16e, 64-512 subcarriers are used in IEEE 802.11ac. In practical situations like these, MC-CSK will perform best in BER performance among the three comparable systems. With superiority in both spectral efficiency and BER performance, the proposed scheme is considered to be a strong candidate for many wireless communication scenarios.

Unfortunately, there is some trade-off here. The performance improvements in MC-CSK can only be supported by the increase of system complexity. Comparing to DCSK, MC-CSK requires extra circuits to implement the MC transmission. That includes a serial-to-parallel circuit and $2M$ multipliers in the transmitter (see Fig. 6). Whereas in the receiver, $2M$ multipliers, $2M$ matched filters, $2M$ switches and one parallel-to-serial circuit are needed (see Fig. 9). In addition, in order to realize multi-level CSK modulation, MC-CSK introduces M M-to-1 multiplexers as well as OCSG in the transmitter, and also replaces the correlation circuits in DCSK receiver by a digital signal processor, as shown in Fig. 9. Both modifications imply that MC-CSK needs more complicated transceiver circuits compared to DCSK. However, the increase of complexity is worthwhile. On one hand, it brings in firmed performance improvements, such as a much higher bit rate, greatly increased spectral efficiency, and much better BER performances (see Fig. 16) in comparison with DCSK. On the other hand, all delay lines required by DCSK transceiver have been eliminated in MC-CSK, making MC-CSK much easier to be implemented in UWB communications.

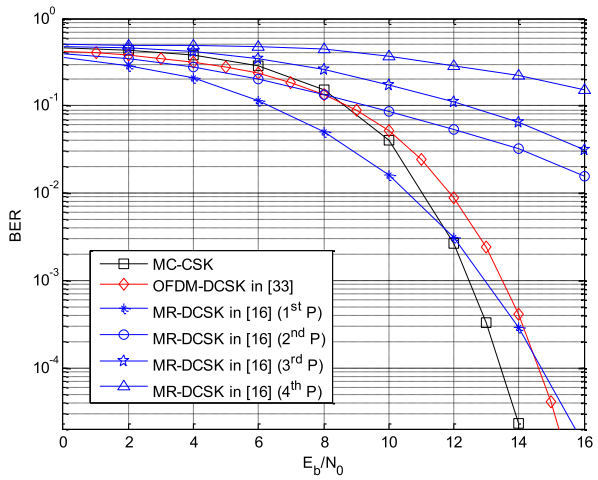

Fig. 17. BER performances of MC-CSK, MR-DCSK in [16] and OFDM-DCSK in [33] over an AWGN channel.

Comparing to MC-DCSK that also involves MC transmission, a slight increase in complexity is noted in MC-CSK. This is due to the following two factors. First, MC-CSK takes advantage of both inphase and quadrature channels. As a result, the number of multipliers in the transmitter has been doubled. Similarly, the numbers of multipliers, matched filters and switches, are also doubled in the receiver. This leads to almost doubled circuit complexity for MC transmission compared to MC-DCSK. But, fortunately, such increases could be avoided if OFDM is employed to implement MC transmission. Second, unlike MC-DCSK, which is based on binary DCSK, MC-CSK with M subcarriers is based on M-ary CSK modulation. As a result, the MC-CSK transmitter utilizes OCSG to generate M chaotic basis signals and to introduce M additional M-to-1 multiplexers to map data symbols into these basis signals. Meanwhile, the number of correlations performed by the DSP in MC-CSK receiver is M times of that in MC-DCSK receiver. For this reason, MC-CSK increases the circuit complexity in the transmitter and the computational complexity in the receiver for multi-level modulation.

In summary, the overall complexity of MC-CSK would be slightly higher than that of MC-DCSK. However, the additional design also makes MC-CSK outperform MC-DCSK in bit rate, spectral efficiency (see Fig. 8) and even BER performance (see Fig. 16).

The BER performances of MC-CSK, MR-DCSK in [16] and OFDM-DCSK in [33] are compared in Fig. 17. All results are obtained with a spreading sequence length of 64, and the number of bits in each symbol is set to 4 for all systems. In OFDM-DCSK, a single-user case is considered and the number of private frequency is 1. In MR-DCSK, the priority vector is set to $[3\pi/10, \pi/10, \pi/25]$. With different protection distances in the constellation, data bits in the MR-DCSK system have dissimilar priorities and thus show unequal BER performances (denoted as '1st P', '2nd P', '3rd P', and '4th P', respectively) in Fig. 17. In contrast, MC-CSK and OFDM-DCSK systems adopt uniformly spaced constellations, but with different protection distances. As a result, the BERs of data bits sent for a symbol in MC-CSK are identical, which also holds true for OFDM-DCSK. In Fig.17, the 1st P data bits in MR-DCSK achieve the best BER performance for low E_b/N_0 levels since they are protected with the largest distance in constellation. Even though the protection distance for data bits in MC-CSK is smaller than that for the 1st P data bits in MR-DCSK, MC-CSK can still outperforms the 1st P data bits in MR-DCSK for high E_b/N_0 levels (i.e., $E_b/N_0 > 12d$B in Fig.17) as more noise-signal cross terms are added into the observation variables in MR-DCSK. Similarly, MC-CSK performs slightly worse than OFDM-DCSK in low E_b/N_0 cases due to the reduction of protection distance generally brought by multi-level CSK modulation, but it outperforms OFDM-DCSK for high E_b/N_0 levels (i.e. $E_b/N_0 > 8d$B in Fig.17) by reducing the noise interferences in decision variables.

Here, the BER performances of MC-CSK are also compared with other two high-data-rate designs, proposed in [24] and [25], which are referred to as HCS-DCSK2 and OM-DCSK hereafter. For a fair comparison, the multi-carrier system based on OM- DCSK is adopted, and the numbers of subcarriers in MC-CSK and multi-carrier OM-DCSK systems are set to be same so that they show identical spectral efficiencies. In all three systems, the number of bits transmitted in each symbol is 4, and the spreading factor is set to 256. Their BER performances over AWGN channels are depicted in Fig. 18. As shown, HCS-DCSK2 performs much worse than the other two systems. This is because HCS-DCSK2 suffers from high interferences as it transmits multiple data-bearing signals in one time slot and then separates them by semi-orthogonal chaotic sequences. It is also noticed that MC-CSK performs the best and its BER performance is about 1dB better than that of multi-carrier OM-DCSK. This performance improvement is attributed to the multi-level modulation based on the Gram-Schmidt algorithm, as the Gram-Schmidt algorithm can remove variations in auto-correlations of chaotic basis signals and therefore reduce the uncertainties in decision variables in MC-CSK.

Although both MC-CSK and HCS-DCSK2 could transmit multiple data bits in one symbol duration, they are based on totally different mechanisms. HCS-DCSK2 is based on the code division multiple access (CDMA) and binary DCSK modulation, while MC-CSK is based on MC transmission and multi-level CSK modulation. These theoretical differences enable MC-CSK to be much easier to implement while obtaining better performances. On one hand, comparing to HCS-DCSK2, MC-CSK removes the circuits for chaotic code synchronization and all delay lines, as it does not employ different chaotic sequences but using different subcarriers to separate the reference and the multiple data-bearing signals. On the other hand, multi-level CSK modulation helps MC-CSK achieve much higher bit rate and better BER performance (see Fig. 18) in comparison with HCS-DCSK2.

With same spectral efficiency, MC-CSK and multi-carrier OM-DCSK may have some similarities in multi-level modulation. However, the reference transmission format and the method to build chaotic basis signals in MC-CSK are unique and differ significantly from those used in multi-carrier OM-DCSK. Firstly, the Gram-Schmidt algorithm, rather than Walsh codes and Hilbert Transform, is used to build the chaotic

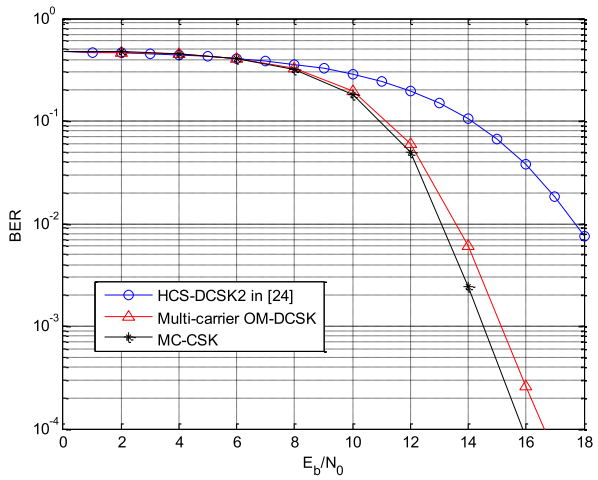

Fig. 18. BER comparison among MC-CSK, HCS-DCSK2 in [24] and the multi-carrier system based on OM-DCSK in [25] over an AWGN channel.

basis signals. These two methods differ in three ways: 1) The Gram-Schmidt algorithm can eliminate variations of auto-correlations of chaotic basis signals, but chaotic basis signals built by Walsh codes and Hilbert Transform still suffer from varying auto-correlations. 2) With the same chaotic sequence length, the Gram-Schmidt algorithm can build much shorter chaotic basis signals, reducing noises in decision variables. 3) Compared to the combination of Walsh codes and Hilbert Transform, the Gram-Schmidt algorithm can be implemented with a lower complexity cost, as it avoids all delay lines, Hilbert filters, as well as circuits for weighting and Walsh code synchronization. As a conclusion, the Gram-Schmidt algorithm facilitates MC-CSK system to achieve better BER performance (see Fig. 18) with simpler transceivers (see Fig. 6 and Fig. 9) in comparison with multi-carrier OM-DCSK. Secondly, MC-CSK transmits all chaotic basis signals to the receiver, while multi-carrier OM-DCSK sends only one chaotic basis signal to the receiver. This helps simplify the receiver of MC-CSK by removing circuits for reconstructing chaotic basis signals as well as avoiding possible performance loss caused by non-ideal recoveries of these basis signals. Based on these two facts, MC-CSK has not only better BER performance but also much lower system complexity in comparison with the multi-carrier OM-DCSK.

V. Conclusion

In this paper, a new MC-CSK system is designed, analyzed and evaluated, in which multi-level CSK modulation is combined with multi-carrier transmission to achieve higher data rate, better spectral efficiency and better performance. To avoid non-zero cross-correlations as well as fluctuations in auto-correlations, the proposed scheme applies the Gram-Schmidt algorithm to segments of chaotic signals to obtain multiple strictly-orthogonal basis signals with fixed energy. These basis signals are shared by multiple modulated signals, each can carry multiple data bits. Being separated by I/Q channels, all references (i.e., the chaotic basis signals) along with multiple data-bearing signals will be sent simultaneously over different subcarriers in the MC-CSK system.

Unlike conventional CSK modulation, the proposed scheme is equipped with the T-R technique so that correlation-based detector could be utilized and no chaos synchronization is required. By transmitting the reference and data-bearing signals simultaneously, MC-CSK removes all delay lines from both the transmitters and the receivers. With multiple bits transmitted over each subcarrier, the spectral efficiency and the data rate are remarkably increased. By reference sharing, the MC-CSK system could achieve better performance in comparison to DCSK and its multi-carrier counterparts in most MC transmission scenarios. Despite that a slightly complicated transceiver circuitry design may be needed, the MC-CSK system brings firmed performance enhancement and unprecedented potential to many high-data-rate communication scenarios.

References

[1] H. Dedieu, M. P. Kennedy, and M. Hasler, "Chaos shift keying: Modulation and demodulation of a chaotic carrier using self-synchronizing Chua's circuits," *IEEE Trans. Circuits Syst. II, Analog Digit. Signal Process*, vol. 40, no. 10, pp. 634–642, Oct. 1993.

[2] F. C. M. Lau and C. K. Tse, "On optimal detection of noncoherent chaos-shift-keying signals in a noisy environment," *Int. J. Bifurcation Chaos*, vol. 13, no. 6, pp. 1587–1597, 2003.

[3] G. Kolumbán, B. Vizváki, W. Schwarz, and A. Abel, "Differential chaos shift keying: A robust coding for chaos communication," in *Proc. NDES*, Seville, Spain, 1996, pp. 87–92.

[4] G. Kolumbán, G. Kis, M. P. Kennedy, and Z. Jáko, "FM-DCSK: A new and robust solution to chaos communications," in *Proc. Int. Symp. Nonlinear Theory Appl.*, Honolulu, HI, USA, 1997, pp. 117–120.

[5] M. Sushchik, L. S. Tsimring, and A. R. Volkovskii, "Performance analysis of correlation-based communication schemes utilizing chaos," *IEEE Trans. Circuits Syst. I, Fundam. Theory Appl.*, vol. 47, no. 12, pp. 1684–1691, Dec. 2000.

[6] G. Kolumbán, "Theoretical noise performance of correlator-based chaotic communications schemes," *IEEE Trans. Circuits Syst. I, Fundam. Theory Appl.*, vol. 47, no. 12, pp. 1692–1701, Dec. 2000.

[7] M. P. Kennedy, G. Kolumbán, G. Kis, and Z. Jako, "Performance evaluation of FM-DCSK modulation in multipath environments," *IEEE Trans. Circuits Syst. I, Fundam. Theory Appl.*, vol. 47, no. 12, pp. 1702–1711, Dec. 2000.

[8] F. C. M. Lau and C. K. Tse, *Chaos-Based Digital Communication Systems*. Berlin, Germany: Springer, 2003, ch. 2.

[9] Z. Galias and G. M. Maggio, "Quadrature chaos-shift keying: Theory and performance analysis," *IEEE Trans. Circuits Syst. I, Fundam. Theory Appl.*, vol. 48, no. 12, pp. 1510–1519, Dec. 2001.

[10] G. Kis, "Performance analysis of chaotic communication systems," Ph.D. dissertation, Dept. Meas. Inf. Syst., Budapest Univ. Tech. Econ. Press, Budapest, Hungary, 2005.

[11] H. Yang and G.-P. Jiang, "High-efficiency differential-chaos-shift-keying scheme for chaos-based noncoherent communication," *IEEE Trans. Circuits Syst. II, Express Briefs*, vol. 59, no. 5, pp. 312–316, May 2012.

[12] T. J. Wren and T. C. Yang, "Orthogonal chaotic vector shift keying in digital communications," *IET Commun.*, vol. 4, no. 6, pp. 739–753, 2010.

[13] H. Yang, G.-P. Jiang, and J. Duan, "Phase-separated DCSK: A simple delay-component-free solution for chaotic communications," *IEEE Trans. Circuits Syst. II, Express Briefs*, vol. 61, no. 12, pp. 967–971, Dec. 2014.

[14] Y. Fang, L. Wang, P. Chen, J. Xu, G. Chen, and W. Xu, "Design and analysis of a DCSK-ARQ/CARQ system over multipath fading channels," *IEEE Trans. Circuits Syst. I, Reg. Papers*, vol. 62, no. 6, pp. 1637–1647, Jun. 2015.

[15] Y. Lyu, L. Wang, G. Cai, and G. Chen, "Iterative receiver for *M*-ary DCSK systems," *IEEE Trans. Commun.*, vol. 63, no. 11, pp. 3929–3936, Nov. 2015.

[16] L. Wang, G. Cai, and G. R. Chen, "Design and performance analysis of a new multiresolution *M*-ary differential chaos shift keying communication system," *IEEE Trans. Wireless Commun.*, vol. 14, no. 9, pp. 5197–5208, Sep. 2015.

[17] A. Kumar and P. R. Sahu, "Performance analysis of differential chaos shift keying modulation with transmit antenna selection," *IET Commun.*, vol. 10, no. 3, pp. 327–335, 2016.
[18] G. Kaddoum, E. Soujeri, and Y. Nijsure, "Design of a short reference noncoherent chaos-based communication systems," *IEEE Trans. Commun.*, vol. 64, no. 2, pp. 680–689, Feb. 2016.
[19] F. J. Escribano, G. Kaddoum, A. Wagemakers, and P. Giard, "Design of a new differential chaos-shift-keying system for continuous mobility," *IEEE Trans. Commun.*, vol. 64, no. 5, pp. 2066–2078, May 2016.
[20] Y. Fang, G. Han, P. Chen, F. C. M. Lau, G. Chen, and L. Wang, "A survey on DCSK-based communication systems and their application to UWB scenarios," *IEEE Commun. Surveys Tuts.*, vol. 18, no. 3, pp. 1804–1837, 3rd Quart., 2016.
[21] M. R. Casu and G. Durisi, "Implementation aspects of a transmitted-reference UWB receiver," *J. Wirel. Commun. Mob. Comput.*, vol. 5, no. 5, pp. 537–549, 2005.
[22] W. K. Xu, L. Wang, and G. Kolumbán, "A novel differential chaos shift keying modulation scheme," *Int. J. Bifurcation Chaos*, vol. 21, no. 03, pp. 799–814, 2011.
[23] W. K. Xu, L. Wang, and G. Kolumbán, "A new data rate adaption communications scheme for code-shifted differential chaos shift keying modulation," *Int. J. Bifurcation Chaos*, vol. 22, no. 8, p. 1250201, 2012.
[24] G. Kaddoum and F. Gagnon, "Design of a high-data-rate differential chaos-shift keying system," *IEEE Trans. Circuits Syst. II, Express Briefs*, vol. 59, no. 7, pp. 448–452, Jul. 2012.
[25] H. Yang, W. K. S. Tang, G. Chen, and G.-P. Jiang, "System design and performance analysis of orthogonal multi-level differential chaos shift keying modulation scheme," *IEEE Trans. Circuits Syst. I, Reg. Papers*, vol. 63, no. 1, pp. 146–156, Jan. 2016.
[26] K. Fazel and S. Kaiser, *Multi-Carrier and Spread Spectrum Systems: From OFDM and MC-CDMA to LTE and WiMAX*, 2nd ed. Hoboken, NJ, USA: Wiley, 2008.
[27] C. Snow, L. Lampe, and R. Schober, "Impact of WiMAX interference on MB-OFDM UWB systems: Analysis and mitigation," *IEEE Trans. Commun.*, vol. 57, no. 9, pp. 2818–2827, Sep. 2009.
[28] N. Abu-Ali, A. M. Taha, M. Salah, and H. Hassanein, "Uplink scheduling in LTE and LTE-advanced: Tutorial, survey and evaluation framework," *IEEE Commun. Surveys Tuts.*, vol. 16, no. 3, pp. 1239–1265, 3rd Quart., 2014.
[29] M. Caus and A. I. Perez-Neira, "Multi-stream transmission for highly frequency selective channels in MIMO-FBMC/OQAM systems," *IEEE Trans. Signal Process.*, vol. 62, no. 4, pp. 786–796, Feb. 2014.
[30] S. Weinstein and P. Ebert, "Data transmission by frequency-division multiplexing using the discrete Fourier transform," *IEEE Trans. Commun. Technol.*, vol. 19, no. 5, pp. 628–634, Oct. 1971.
[31] J. A. C. Bingham, "Multicarrier modulation for data transmission: An idea whose time has come," *IEEE Commun. Mag.*, vol. 28, no. 5, pp. 5–14, May 1990.
[32] G. Kaddoum, F. Richardson, and F. Gagnon, "Design and analysis of a multi-carrier differential chaos shift keying communication system," *IEEE Trans. Commun.*, vol. 61, no. 8, pp. 3281–3291, Aug. 2013.
[33] G. Kaddoum, "Design and performance analysis of a multiuser OFDM based differential chaos shift keying communication system," *IEEE Trans. Commun.*, vol. 64, no. 1, pp. 249–260, Jan. 2016.
[34] G. Kaddoum and F. Shokraneh, "Analog network coding for multi-user multi-carrier differential chaos shift keying communication system," *IEEE Trans. Wireless Commun.*, vol. 14, no. 3, pp. 1492–1505, Mar. 2015.
[35] K. J. Horadam, *Hadamard Matrices and Their Applications*. Princeton, NJ, USA: Princeton Univ. Press, 2006.
[36] T. J. Wren, "Orthogonal chaotic vector shift keying in digital communications," Ph.D. dissertation, Dept. Eng. Design, Univ. Sussex, Brighton, U.K., Jun. 2007.
[37] A. Wolf, J. B. Swift, H. L. Swinney, and J. A. Vastano, "Determining Lyapunov exponents from a time series," *Phys. D, Nonlinear Phenomena*, vol. 16, no. 3, pp. 285–317, 1985.
[38] Y. Jing, F. Yin, and Z. Chen, "An H_∞ filter based approach to combat inter-carrier interference for OFDM systems," *IEEE Commun. Lett.*, vol. 12, no. 6, pp. 453–455, Jun. 2008.
[39] L. Wu, X. D. Zhang, P. S. Li, and Y.-T. Su, "A blind CFO estimator based on smoothing power spectrum for OFDM systems," *IEEE Trans. Commun.*, vol. 57, no. 7, pp. 1924–1927, Jul. 2009.
[40] S. U. Hwang, J. H. Lee, and J. Seo, "Low complexity iterative ICI cancellation and equalization for OFDM systems over doubly selective channels," *IEEE Trans. Broadcast.*, vol. 55, no. 1, pp. 132–139, Mar. 2009.
[41] S. Benedetto and E. Biglieri, *Principles of Digital Transmission: With Wireless Applications*. Norwell, MA, USA: Kluwer, 1999.
[42] T. Rappaport, *Wireless Communications: Principles and Practice*, 2nd ed. Englewood Cliffs, NJ, USA: Prentice-Hall, 2001.
[43] Y. Xia, C. K. Tse, and F. C. M. Lau, "Performance of differential chaos-shift-keying digital communication systems over a multipath fading channel with delay spread," *IEEE Trans. Circuits Syst. II, Express Briefs*, vol. 51, no. 12, pp. 680–684, Dec. 2004.
[44] S. Haykin, *Communication Systems*. Hoboken, NJ, USA: Wiley, 1994.
[45] J. G. Proakis, *Digital Communications*. New York, NY, USA: McGraw-Hill, 1995.

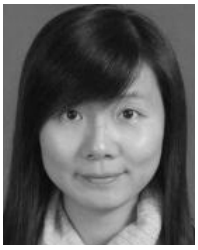

Hua Yang (M'16) received the B.E. degree in automation and the Ph.D. degree in information and communication engineering from the Nanjing University of Posts and Telecommunications, China, in 2003 and 2014, respectively. Since 2014, she has been an Assistant Professor with the School of Electronic Science and Engineering, Nanjing University of Posts and Telecommunications. In 2016, she was a Post-Doctoral Fellow with the Department of Electronic Engineering, City University of Hong Kong. Her current research interests include nonlinear circuits and systems and chaos-based communications.

Wallace K. S. Tang (M'96–SM'09) received the Ph.D. degree from the City University of Hong Kong in 1996. He is currently an Associate Professor with the Department of Electronic Engineering, City University of Hong Kong. He has authored over 100 journal papers, eight book chapters, and three books, focusing on nonlinear systems, evolutionary algorithms, and complex networks. He is currently an Associate Editor of the IEEE TRANSACTIONS ON CIRCUITS AND SYSTEMS II and the *International Journal of Bifurcation and Chaos*.

Guanrong Chen (M'89–SM'92–F'97) was a Tenured Full Professor with the University of Houston, TX, USA. He has been a Chair Professor and the Director of the Centre for Chaos and Complex Networks, City University of Hong Kong, since 2000. He is a Highly Cited Researcher in Engineering and in Mathematics according to Thomson Reuters. He is a member of the Academy of Europe and a fellow of The World Academy of Sciences. He received the 2011 Euler Gold Medal, Russia, and conferred Honorary Doctorate by the Saint Petersburg State University, Russia, in 2011, and the University of Le Havre, France, in 2014.

Guo-Ping Jiang (M'03–SM'16) received the Ph.D. degree in control theory and engineering from Southeast University, Nanjing, China, in 1997. He is currently a Professor and the Vice President with the Nanjing University of Posts and Telecommunications, Nanjing, China. He has authored or coauthored over 200 published articles and two books in the area of nonlinear systems and control. His current research interests include chaos synchronization and control, chaos-based communication, and complex dynamical networks. He received the Awards for the New Century Excellent Talents of the Ministry of Education, China, in 2006, and the Awards for the 333 Project High-level Talents of Jiangsu Province, China, in 2011.